Analytical solution of the radiative transfer equation for infinite-space fluence

André Liemert and Alwin Kienle
Institut für Lasertechnologien in der Medizin und Meßtechnik, Helmholtzstrasse 12, D-89081 Ulm, Germany
(Received 22 July 2010; published 21 January 2011)

This Brief Report presents the derivation of analytical expressions for the fluence of the steady state radiative transfer equation in an infinitely extended and anisotropically scattering medium in arbitrary dimensions for different source types. The fluence, which is composed of an infinite sum of diffusion-like Green's functions, was compared to the Monte Carlo method. Within the stochastic nature of the Monte Carlo simulations, an exact agreement was found in the steady state and time domains. It is shown that the use of low-order approximations is sufficient for many relevant cases.

DOI: 10.1103/PhysRevA.83.015804 PACS number(s): 42.25.Dd

The radiative transfer equation (RTE) is used in many different fields in physics such as astrophysics, climate research, and biophotonics [1,2]. It is considered as the gold standard for calculation of light propagation in random media, for example, biological tissue, because it is for many cases a valid approximation of the Maxwell equations [3,4], avoiding the high demand for computer power needed for solving the Maxwell equations. However, analytical solutions are known only for the case of isotropic scattering [5–7]. Thus numerical methods, especially Monte Carlo simulations, are applied to solve the radiative transfer equation.

We derive analytical solutions of the radiative transfer equation for anisotropic scattering. The derived solutions enable a simple implementation and can be evaluated many orders of magnitude ($\approx 10^{10}$) faster than Monte Carlo simulations. Expressions of the fluence for isotropically emitting point, spherical-shell, and cylincrical-shell sources in infinitely extended random media are obtained from the steady state radiative transfer equation in all dimensions. These sources and geometry are important, for example, for interstitial measurements during laser therapy [8] and neutron transport theory [9,10]. Solutions in the time domain are obtained via Fourier transform. In both domains, the solutions are compared with Monte Carlo simulations. The derived fluence represents the particular solution and enables the implementation of boundary conditions, for example, for a semi-infinite geometry in combination with the homogeneous solution.

The planar-geometry version of the radiative transfer equation for the radiance $\psi(x,\tau)$ in the steady state domain is given by [11]

$$\tau\frac{\partial}{\partial x}\psi(x,\tau)+\mu_t\psi(x,\tau)=\mu_s\int_{-1}^{1}f(\tau,\tau')\psi(x,\tau')d\tau'+\frac{S(x)}{2}, \tag{1}$$

where

$$f(\tau,\tau')=\sum_{n=0}^{\infty}\frac{2n+1}{2}f_nP_n(\tau)P_n(\tau'). \tag{2}$$

Here μ_s is the scattering coefficient, μ_a is the absorption coefficient, $\mu_t=\mu_a+\mu_s$ is the total interaction coefficient, P_n are the Legendre polynomials, and τ is the cosine of the angle between the direction of propagation and unit vector oriented along the x axis. The expansion coefficients for an azimuthally independent phase function are given by

$$f_n=\int_{-1}^{1}f(\tau)P_n(\tau)d\tau. \tag{3}$$

In the case of the Henyey-Greenstein function, they are obtained by $f_n=g^n\ \forall\ n\in\mathbb{N}_0$ with the anisotropy factor g. The internal isotropic light source density is denoted as $S(x)$. Expanding the radiance in Legendre polynomials,

$$\psi(x,\tau)=\sum_{n=0}^{\infty}\frac{2n+1}{2}\phi_n(x)P_n(\tau), \tag{4}$$

leads to an infinite set of ordinary differential equations for $n=0,1,\ldots,N$ (N odd and $N\to\infty$) [9]:

$$\frac{n+1}{2n+1}\frac{d}{dx}\phi_{n+1}(x)+\frac{n}{2n+1}\frac{d}{dx}\phi_{n-1}(x)+\mu_{an}\phi_n(x)=S(x)\delta_{n,0}, \tag{5}$$

where $\mu_{an}=\mu_a+(1-f_n)\mu_s$ are the absorption coefficients of order n and $\phi_{-1}=\phi_{N+1}=0$. The solutions of this system are the Legendre moments $\phi_n(x)$. The fluence corresponds to the isotropic component of the radiance $\psi(x,\tau)$ and is given by the lowest order Legendre moment $\phi_0(x)$. The source distribution $S(x)=\delta(x)$ is used for obtaining the Green's function. In order to solve Eq. (5), we applied the plane wave expansion for the Legendre moments

$$\phi_n(x)=\frac{1}{2\pi}\int_{-\infty}^{\infty}\phi_n(k)e^{ikx}dk, \tag{6}$$

and, for the source distribution,

$$\delta(x)=\frac{1}{2\pi}\int_{-\infty}^{\infty}e^{ikx}dk, \tag{7}$$

which yields a system of $N+1$ linear equations:

$$\frac{n+1}{2n+1}ik\phi_{n+1}(k)+\frac{n}{2n+1}ik\phi_{n-1}(k)+\mu_{an}\phi_n(k)=\delta_{n,0}. \tag{8}$$

In matrix notation, Eq. (8) becomes

$$\mathbf{T}[\phi_0(k),\phi_1(k),\ldots,\phi_N(k)]^T=[1,0,\ldots,0]^T, \tag{9}$$

with a symmetric tridiagonal system matrix

$$\mathbf{T} = \begin{pmatrix} \mu_a & ik & 0 & 0 & \cdots & 0 \\ ik & 3\mu_{a1} & i2k & 0 & \cdots & \vdots \\ 0 & i2k & \ddots & \ddots & \cdots & 0 \\ 0 & 0 & \ddots & \ddots & \ddots & 0 \\ \vdots & \cdots & \cdots & \ddots & \ddots & iNk \\ 0 & \cdots & 0 & 0 & iNk & (2N+1)\mu_{aN} \end{pmatrix} \tag{10}$$

Using Cramer's rule,

$$\phi_0(k) = \frac{\det(\mathbf{T}_0)}{\det(\mathbf{T})}, \tag{11}$$

where $\mathbf{T}_0$ is a symmetric tridiagonal matrix obtained by replacing the first column of $\mathbf{T}$ by the vector $[1,0,\cdots,0]^T$; $\phi_0(k)$ is derived and can be rewritten in the form

$$\phi_0(k) = \sum_{i=1}^{\frac{N+1}{2}} \frac{A_i}{k^2+\nu_i^2}. \tag{12}$$

The values of A_i and ν_i are found as follows. By setting $\mathcal{D}_0(\lambda) = 0$ and $\mathcal{D}_1(\lambda) = 1$, the use of the recursively defined polynomials for $n = 1,\ldots,N$,

$$\mathcal{D}_{n+1}(\lambda) = (2n+1)\mu_{an}\mathcal{D}_n(\lambda) + \lambda n^2 \mathcal{D}_{n-1}(\lambda), \tag{13}$$

leads to the first polynomial $P(\lambda)$:

$$P(\lambda) = \mathcal{D}_{N+1}(\lambda) = \sum_{l=0}^{\frac{N-1}{2}} a_l \lambda^l. \tag{14}$$

For $\mathcal{D}_0(\lambda) = 1$ and $\mathcal{D}_1(\lambda) = \mu_a$, Eq. (13) defines the second polynomial $Q(\lambda)$ as

$$Q(\lambda) = \mathcal{D}_{N+1}(\lambda) = \sum_{l=0}^{\frac{N+1}{2}} b_l \lambda^l. \tag{15}$$

Note that the characteristic polynomial $p(\kappa)$ needed for the homogeneous solution is also given by setting $p(\kappa) = Q(-\kappa^2)$. The polynomial equation $Q(\lambda) = 0$ gives, all in all, $(N+1)/2$ negative real-valued zeros λ_i. These zeros are used for defining the values $\nu_i = \sqrt{-\lambda_i}$. The coefficients A_i are determined as

$$A_i = \frac{1}{b_{\frac{N+1}{2}}} \frac{P(\lambda_i)}{\prod_{n=1,n\neq i}^{\frac{N-1}{2}} (\lambda_i - \lambda_n)}. \tag{16}$$

The Green's function of the one-dimensional diffusion equation in plane wave expansion is [12]

$$G(x) = \frac{e^{-\nu_1|x|}}{2D\nu_1} = \frac{1}{2\pi D}\int_{-\infty}^{\infty} \frac{e^{ikx}}{k^2+\nu_1^2}\,dk, \tag{17}$$

where $D = 1/(3\mu_{a1})$ denotes the diffusion coefficient. Thus the fluence of the one-dimensional P_N equations becomes

$$\phi_0(x) = \sum_{i=1}^{\frac{N+1}{2}} \frac{A_i}{2} \frac{e^{-\nu_i|x|}}{\nu_i}. \tag{18}$$

Using [13]

$$\phi_0(r) = -\frac{1}{2\pi r}\frac{d}{dx}\phi_0(x)\Big|_{x=r}, \tag{19}$$

the three-dimensional fluence is found from Eq. (18) as

$$\phi_0(r) = \sum_{i=1}^{\frac{N+1}{2}} A_i \frac{e^{-\nu_i r}}{4\pi r}. \tag{20}$$

Therefore the exact solution of the radiative transfer equation for the fluence is an infinite sum of diffusion-like Green's functions. The fluence caused by an isotropic line source is obtained via integration of Eq. (20) over one spatial dimension as

$$\phi_0(\rho) = \int_{-\infty}^{\infty} \phi_0(\rho,z)dz = \sum_{i=1}^{\frac{N+1}{2}} \frac{A_i}{2\pi} K_0(\nu_i\rho). \tag{21}$$

The fluence for an arbitrary dimension s is obtained as

$$\phi_0^{(s)}(|\mathbf{x}|) = \sum_{i=1}^{\frac{N+1}{2}} \frac{A_i}{(2\pi)^{s/2}} \left(\frac{\nu_i}{|\mathbf{x}|}\right)^{\frac{s}{2}-1} K_{s/2-1}(\nu_i|\mathbf{x}|), \tag{22}$$

where $|\mathbf{x}| = \sqrt{x_1^2 + x_2^2 + \cdots + x_s^2}$ and $K_\nu(x)$ is the second kind of modified Bessel function of νth order.

We derived the solutions of the RTE for an isotropic spherical and cylindrical shell source with radii r_s and ρ_s, respectively, as

$$\phi_{\text{sph}}(r) = \frac{1}{8\pi r r_s} \sum_{i=1}^{\frac{N+1}{2}} \frac{A_i}{\nu_i}(e^{-\nu_i|r-r_s|} - e^{-\nu_i|r+r_s|}), \tag{23}$$

$$\phi_{\text{cyl}}(\rho) = \frac{1}{2\pi} \sum_{i=1}^{\frac{N+1}{2}} A_i I_0(\nu_i\rho_<) K_0(\nu_i\rho_>), \tag{24}$$

where $\rho_< = \min\{\rho,\rho_s\}$, $\rho_> = \max\{\rho,\rho_s\}$, and $I_0(x)$ is the modified Bessel function of the first kind.

For the time-dependent case, Eq. (5) becomes a system of partial differential equations:

$$\left(\frac{1}{c}\frac{\partial}{\partial t} + \mu_{an}\right)\phi_n(x,t) + \frac{n+1}{2n+1}\frac{\partial}{\partial x}\phi_{n+1}(x,t) + \frac{n}{2n+1}\frac{\partial}{\partial x}\phi_{n-1}(x,t) = S(x,t)\delta_{n,0}, \tag{25}$$

where c is the speed of light. Solutions of this system can be obtained using complex-valued nth-order absorption coefficients $\mu_{an} = \mu_a + (1-f_n)\mu_s + i\omega/c$ and by performing the inverse Fourier transform [14,15]. In general, for many relevant cases, approximations until order $N = 7$ lead to, practically, the same results as the exact solution. For orders $N \leqslant 7$, the zeros can be obtained analytically. For the case of $N = 7$, the zeros of the fourth-order polynomial obtained from Eq. (15),

$$\lambda^4 + \alpha\lambda^3 + \beta\lambda^2 + \gamma\lambda + \varepsilon = 0, \tag{26}$$

where $\alpha = b_3/b_4$, $\beta = b_2/b_4$, $\gamma = b_1/b_4$, $\varepsilon = b_0/b_4$, are given explicitly. First, any real-valued zero of the cubic equation

$$s^3 - \tfrac{1}{2}\beta s^2 + \tfrac{1}{4}(\alpha\gamma - 4\varepsilon)s + \tfrac{1}{8}\varepsilon(4\beta - \alpha^2) - \tfrac{1}{8}\gamma^2 = 0 \tag{27}$$

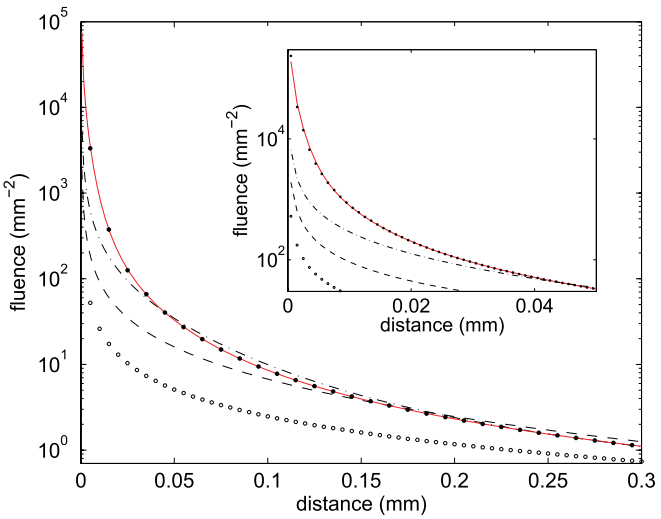

FIG. 1. (Color online) Steady state fluence in an infinite medium for an isotropic point source obtained from the Monte Carlo method (solid circles) and different orders of the analytical solution. The open circles represent the diffusion theory; the dashed curve, the dash-dotted curve, and the solid curve are generated by the P_3, P_7, and P_{39} equations, respectively. The optical properties are $\mu_s' = 1.0$ mm^{-1}, $\mu_a = 0.1$ mm^{-1}, and $g = 0.9$. The inset shows the same curves for smaller distances.

is determined. By setting

$$p = \tfrac{1}{12}\beta^2 - \tfrac{1}{4}(\alpha\gamma - 4\varepsilon),$$
$$q = -\tfrac{1}{108}\beta^3 + \tfrac{1}{24}\beta(\alpha\gamma - 4\varepsilon) + \tfrac{1}{8}\varepsilon(4\beta - \alpha^2) - \tfrac{1}{8}\gamma^2, \quad (28)$$

Cardano's formula [16] leads to the root

$$s = 2\sqrt{\frac{p}{3}}\cos\left(\frac{\varphi}{3}\right) + \frac{\beta}{6}, \quad (29)$$

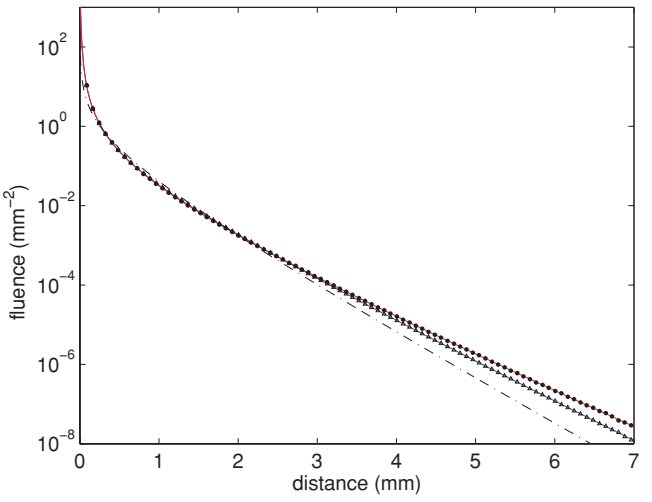

FIG. 2. (Color online) Steady state fluence vs distance from the isotropic point source for two different anisotropy factors. The symbols are data points generated by the Monte Carlo method, and the solid curves are generated by the P_5 equations. The filled circles are calculated for $g = 0.9$ and the open triangles for $g = 0$. The diffusion theory is shown by the dash-dotted curve. The optical properties are $\mu_s' = 1.0$ mm^{-1} and $\mu_a = 1.0$ mm^{-1}.

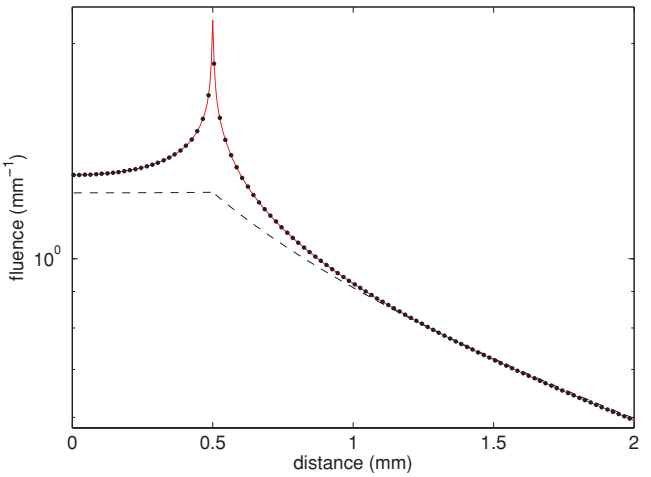

FIG. 3. (Color online) Steady state fluence vs distance from the cylindrical shell source with diameter 1 mm. The optical properties are $\mu_s' = 1.0$ mm^{-1}, $\mu_a = 0.01$ mm^{-1}, and $g = 0.9$.

where

$$\varphi = \arccos\left(-\frac{3q}{2p}\sqrt{\frac{3}{p}}\right). \quad (30)$$

Finally, the values

$$a_{1(2)} = (\alpha \pm \sqrt{8s + \alpha^2 - 4\beta})/2$$
$$b_{1(2)} = s \pm (\alpha s - \gamma)(8s + \alpha^2 - 4\beta)^{-1/2} \quad (31)$$

are used for solving two quadratic equations

$$\lambda^2 + a_i\lambda + b_i = 0, \quad i = 1,2 \quad (32)$$

to find the four required zeros of Eq. (26).

The derived analytical solutions were compared with Monte Carlo simulations [2], which are in the limit of an infinitely

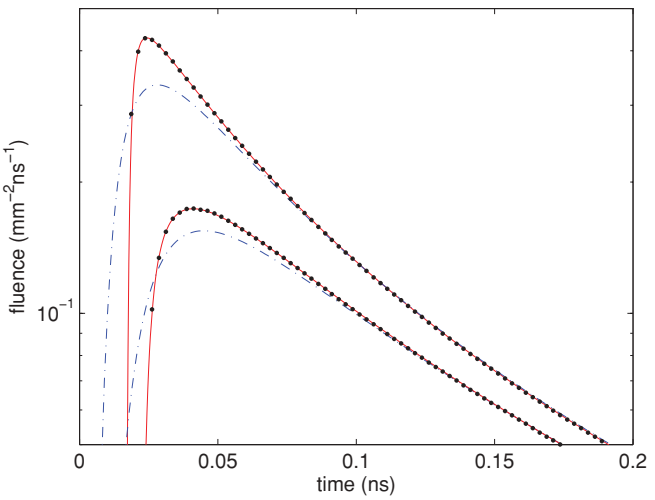

FIG. 4. (Color online) Time-resolved fluence calculated with the Monte Carlo method (solid circles) and the P_7 equations (solid curves). The dash-dotted curves are obtained by diffusion theory. The optical properties are $\mu_s' = 1.0$ mm^{-1}, $\mu_a = 0.01$ mm^{-1}, and $g = 0.9$. The upper curves present the fluence at distance $r = 3.5$ mm and the lower curves at distance $r = 4.5$ mm.

large number of simulated photons, an exact solution of the radiative transfer equation. The Henyey-Greenstein function was used for the analytical solutions and in the Monte Carlo simulations. Figure 1 shows the fluence versus distance from the isotropic point source in an infinitely extended medium obtained from the diffusion theory, the P_N equations ($N = 3,7,39$), and the Monte Carlo method for relatively small distances. It can be seen that the derived expressions converge to the exact solution of the radiative transfer equation. While the diffusion theory has large differences to Monte Carlo simulations, we found for the P_{39} solution relative differences in the range of 3×10^{-5} because of the Monte Carlo noise, which is caused by the finite number of calculated photons ($\approx 4 \times 10^9$).

Figure 2 shows the steady state fluence for two different anisotropy factors calculated with the Monte Carlo method, the P_5 solution, and the diffusion equation. The comparison with the Monte Carlo results shows that, also, the dependence of the fluence on the anisotropy factor is accurately described with the derived equations. Interestingly, large differences of the fluence are obtained for different g values because of the relatively large absorption coefficient.

Figure 3 shows the fluence caused by a cylindrical shell source versus the distance perpendicular to the cylinder axis. The solution calculated with Eq. (24) (solid curve) agrees perfectly with the corresponding Monte Carlo simulation (solid circles), whereas diffusion theory (dashed curve) performs much worse.

The time-resolved fluence for two different distances obtained from Monte Carlo simulations and the P_1 and P_7 equations are shown in Fig. 4. Again, the derived equations are in excellent agreement with the Monte Carlo simulations. In addition, as the distances are larger compared to those shown in Fig. 1, already, the P_7 solution delivers practically exact results. The relative difference between the P_7 and P_{35} equations for this case are in the range of 10^{-7}, whereas diffusion theory has large differences compared to Monte Carlo simulations.

In conclusion, we derived solutions of the radiative transfer equation for the steady state fluence in arbitrary dimensions. The derived solutions were compared with Monte Carlo simulations. Within the stochastic nature of the Monte Carlo method, an exact agreement was found in the steady state and time domains. We note that we provide a MATLAB script for calculation of the fluence on the Internet [17]. In many relevant cases, low-order approximations of the derived solutions are almost exact. For the P_7 approximation, we gave analytical formulas for the zeros; for the P_5 approximation, the zeros can be calculated from our earlier publication [18]. Future important steps are the derivation of the radiance and the inclusion of the exact boundary conditions for obtaining the solution of finite geometries.

[1] A. Ishimaru, *Wave Propagation and Scattering in Random Media* (Academic Press, New York, 1978).

[2] A. Kienle and R. Hibst, Phys. Rev. Lett. **97**, 018104 (2006).

[3] M. I. Mishchenko, L. D. Travis, and A. A. Lacis, *Multiple Scattering of Light by Particles* (Cambridge University Press, New York, 2006).

[4] F. Voit, J. Schäfer, and A. Kienle, Opt. Lett. **34**, 2593 (2009).

[5] V. A. Markel, Waves in Random and Complex Media **14**, 13 (2004).

[6] J. C. J. Paasschens, Phys. Rev. E **56**, 1135 (1997).

[7] F. Martelli, S. Del Bianco, A. Ismaelli, and G. Zaccanti, *Light Propagation through Biological Tissue* (SPIE Press, Bellingham, 2010).

[8] L. C. L. Chin, B. Lloyd, W. M. Whelan, and I. A. Vitkin, J. Appl. Phys. **105**, 102025 (2009).

[9] K. M. Case and P. F. Zweifel, *Linear Transport Theory* (Addison-Wesley, New York, 1967).

[10] J. J. Duderstadt and W. R. Martin, *Transport Theory* (Wiley, New York, 1979).

[11] A. D. Klose and E. W. Larsen, J. Comput. Phys. **220**, 441 (2006).

[12] A. Liemert and A. Kienle, Opt. Express **18**, 9266 (2010).

[13] E. L. Hull and T. H. Forster, J. Opt. Soc. Am. A **18**, 584 (2001).

[14] J. Bouza-Domínguez, Y. Bérubé-Lauzière, and V. Issa, Appl. Opt. **49**, 1414 (2010).

[15] M. Chu, K. Vishwanath, A. D. Klose, and H. Dehghani, Phys. Med. Biol. **54**, 2493 (2009).

[16] T. Frey and M. Bossert, *Signal- und Systemtheorie* (B. G. Teubner, Wiesbaden, 2004).

[17] [http://www.uni-ulm.de/ilm/index.php?id=10020200].

[18] A. Liemert and A. Kienle, Opt. Lett. **35**, 3507 (2010).